Human Reproduction, pp. 1–16, 2018
doi:10.1093/humrep/dey045

human reproduction

ORIGINAL ARTICLE ***Infertility***

Ceramide-1-phosphate has protective properties against cyclophosphamide-induced ovarian damage in a mice model of premature ovarian failure

Natalia Pascuali[1], Leopoldina Scotti[1], Mariana Di Pietro[1], Gonzalo Oubiña[1], Diana Bas[1], María May[2], Antonio Gómez Muñoz[3], Patricia S. Cuasnicú[1], Débora J. Cohen[1], Marta Tesone[1], Dalhia Abramovich[1], and Fernanda Parborell[1,*]

[1]IInstituto de Biología y Medicina Experimental (IByME-CONICET), Vuelta de Obligado 2490, C1428ADN, Buenos Aires, Argentina [2]Instituto de Investigaciones Farmacológicas (ININFA-UBA-CONICET), Facultad de Farmacia y Bioquímica, Universidad de Buenos Aires, Buenos Aires, Argentina [3]Department of Biochemistry and Molecular Biology, Faculty of Science and Technology, University of the Basque Country (UPV/EHU), Bilbao, Spain

*Correspondence address. Instituto de Biología y Medicina Experimental (IByME-CONICET), Vuelta de Obligado 2490, C1428ADN, Buenos Aires, Argentina. Tel: +54-11-47-83-2869; Fax: +54-11-47-86-2564; E-mail: fparborell@gmail.com

Submitted on June 25, 2017; resubmitted on February 12, 2018; accepted on February 13, 2018

STUDY QUESTION: Is ceramide-1-phosphate (C1P) an ovarian protective agent during alkylating chemotherapy?

SUMMARY ANSWER: Local administration of C1P drastically reduces ovarian damage induced by cyclophosphamide (Cy) via protection of follicular reserve, restoration of hormone levels, inhibition of apoptosis and improvement of stromal vasculature, while protecting fertility, oocyte quality and uterine morphology.

WHAT IS KNOWN ALREADY: Cancer-directed therapies cause accelerated loss of ovarian reserve and lead to premature ovarian failure (POF). Previous studies have demonstrated that C1P regulates different cellular processes including cell proliferation, cell migration, angiogenesis and apoptosis. This sphingolipid may be capable of modulating vascular development and apoptosis in ovaries affected by chemotherapy.

STUDY DESIGN, SIZE, DURATION: The 6–8-week-old mice were weighed and administered either a single intraperitoneal injection of Cy (75 mg/kg) or an equal volume of saline solution only for control mice. Control and Cy mice underwent sham surgery and received an intrabursal injection of saline solution, while Cy + C1P animal groups received 5 µl C1P, either 0.5 or 1 mM, under the bursa of both ovaries 1 h prior to Cy administration.

PARTICIPANTS/MATERIALS, SETTING, METHODS: Animals were euthanized by cervical dislocation or cardiac puncture 2 weeks after surgery for collection of blood orovary and uterus samples, which were cleaned of adhering tissue in culture medium and used for subsequent assays. Ovaries were used for Western blotting or immunohistochemical and/or histological analyses or steroid extraction, as required (n = 5–8 per group). A set of mice (n = 3/group) was destined for oocyte recovery and IVF. Finally, another set (n = 5–6/group) was separated to study fertility parameters.

MAIN RESULTS AND THE ROLE OF CHANCE: The number of primordial ($P < 0.01$), primary ($P < 0.05$) and preantral follicles ($P < 0.05$) were decreased in Cy-treated mice compared to control animals, while atretic follicles were increased ($P < 0.001$). In Cy + C1P mice, the ovaries recovered control numbers of these follicular structures, in both C1P doses studied. Cy affected AMH expression, while it was at least partially recovered when C1P is administered as well. Cy caused an increase in serum FSH concentration ($P < 0.01$), which was prevented by C1P coadministration ($P < 0.01$). E2 levels in Cy-treated ovaries decreased significantly compared to control ovaries ($P < 0.01$), whilst C1P restored E2 levels to those of control ovaries ($P < 0.01$). Cy increased the expression of BAX ($P < 0.01$) and decreased the expression of BCLX-L compared to control ovaries ($P < 0.01$). The ovarian BCLX-L:BAX ratio was also lower in Cy-treated mice ($P < 0.05$).

In the Cy + C1P group, the expression levels of BAX, BCLX-L and BCLX-L:BAX ratio were no different than those in control ovaries. In addition, acid sphingomyelinase (A-SMase) expression was higher in Cy-treated ovaries, whilst remaining similar to the control in the Cy + C1P group. Cy increased the apoptotic index (TUNEL-positive follicles/total follicles) in preantral and early antral stages, compared to control ovaries ($P < 0.001$ and $P < 0.01$, respectively). C1P protected follicles from this increase. No primordial or primary follicular cells stained for either cleaved caspase-3 or TUNEL when exposed to Cy, therefore, we have found no evidence for follicular reserve depletion in response to Cy being due to apoptosis. Cy caused evident vascular injury, especially in large cortical stromal vessels, and some neovascularization. In the Cy + C1P group, the disruptions in vascular wall continuity were less evident and the number of healthy stromal blood vessels seemed to be restored. In Cy-treated ovaries α-SMA-positive cells showed a less uniform distribution around blood vessels. C1P coadministration partially prevented this Cy-induced effect, with a higher presence of α-SMA-positive cells surrounding vessels. By H&E staining, Cy-treated mice showed endometrial alterations compared to controls, affecting both epithelial and stromal compartments. However, C1P allowed that the stromal tissue to maintain its loose quality and its glandular branches. Cy-treated animals had significantly lower pregnancy rates and smaller litter sizes compared with control mice ($P = 0.013$ and $P < 0.05$, respectively), whereas cotreatment with C1P preserved normal fertility. Furthermore, a higher ($P < 0.05$) proportion of abnormal oocytes was recovered from Cy-treated mice compared to the control, which was prevented by C1P administration.

LARGE SCALE DATA: N/A.

LIMITATIONS REASONS FOR CAUTION: The results of this study were generated from an *in-vivo* animal experimental model, already used by several authors. Further studies on C1P functions in female reproduction in pathological conditions such as chemotherapy-induced ovarian failure and on the safety of use of this sphingolipid are required.

WIDER IMPLICATIONS OF THE FINDINGS: The present findings showed that C1P administration prior to Cy might be a promising fertility preservation strategy in female patients who undergo chemotherapy.

STUDY FUNDING/COMPETING INTEREST(S): This work was supported by grants from ANPCyT (PICT 2015-1117), CONICET (PIP 380), Cancer National Institute (INC) and Roemmers Foundation, Argentina. The authors declare no conflicts of interest.

Key words: ovarian reserve / sphingolipids / chemotherapy / gonadotoxicity / oncofertility

Introduction

Recent advances in cancer management have raised survival rates of both adult and paediatric patients. Still, the deleterious effects of antitumoral treatments on female fertility remain to be addressed. The risk of gonadal damage depends on factors such as the chemotherapy protocol, the total administered dose and the age and amount of ovarian reserve of the patient at the time of treatment (Wallace and Kelsey, 2010; Sanchez *et al.*, 2013).

Primordial follicles represent the ovarian reserve and decline throughout reproductive age. Cancer-directed therapies can cause accelerated loss of ovarian reserve and atrophy, leading to premature ovarian failure (POF, also termed premature ovarian insufficiency (POI)). (Himelstein-Braw *et al.*, 1978; Familiari *et al.*, 1993; Oktem and Oktay, 2007). The effects of antitumoral therapies on the ovaries can be assessed through the measurement of different markers, including serum early phase FSH, estradiol and anti-Mullerian hormone (AMH) levels, the presence of amenorrhoea and antral follicle count.

Ovarian follicles have high susceptibility to apoptosis induced by many chemotherapic drugs (Perez *et al.*, 1997). Cyclophosphamide (Cy), an alkylating drug used in chemotherapeutic protocols for cancer and immune diseases, presents the highest impact on female fertility (Meirow and Nugent, 2001; Mark-Kappeler *et al.*, 2011). It causes progressive and irreversible damage by destruction of oocytes, follicular depletion and severe vascular damage in the ovary (Ataya *et al.*, 1988; Pydyn and Ataya, 1991). Several studies have recently evaluated the cellular mechanism by which chemotherapic drugs affect ovarian reserve. In particular, these studies have analysed the role of TAp63 as an inducer of apoptosis in the oocytes and reported fertoprotective adjuvants that counteract Tap63 (Gonfloni *et al.*, 2009; Kim *et al.*, 2015; Rossi *et al.*, 2017).

Ovarian protective drugs administered prior and during the chemotherapy might preserve the fertility in young children, adolescents and adult female cancer survivors. GnRH agonists have been used as in attempt to reduce gonadotoxicity by down-regulation of FSH and LH secretion from the pituitary gland and its consequent inhibition of follicular recruitment (Blumenfeld and von Wolff, 2008). Nevertheless, several studies have shown contradictory results regarding the use of GnRH agonists to prevent gonadotoxic damage in the ovary (Bildik *et al.*, 2015; Blumenfeld *et al.*, 2015). Accordingly, more studies are required to find new candidates as fertoprotective agents against chemotherapy.

Sphingolipids are involved in the regulation of death, proliferation, migration and angiogenesis, among other cellular functions (Maceyka *et al.*, 2002; Gangoiti *et al.*, 2010; Ouro *et al.*, 2014; Qi *et al.*, 2010). The major bioactive sphingolipid metabolites include sphingosine, ceramide, sphingosine-1-phosphate (S1P) and ceramide-1-phosphate (C1P). We and several authors have demonstrated that S1P and C1P are key mediators in the processes of apoptosis and angiogenesis in different tissues, in both physiological and pathological conditions (Cuvillier *et al.*, 1996; Arana *et al.*, 2010; Rivera *et al.*, 2015; Di Pietro *et al.*, 2017; Scotti *et al.*, 2016).

Several data have demonstrated that apoptosis and altered angiogenesis could be responsible for the damage of ovarian follicles induced by chemotherapeutic agents (Meirow and Nugent, 2001; Meirow *et al.*, 2001). In particular, in the reproductive system, several

studies have shown that S1P protects ovarian follicles and oocytes from irradiation and chemotherapy-induced apoptosis (Morita and Tilly, 2000; Morita *et al.*, 2000; Jurisicova *et al.*, 2006; Hancke *et al.*, 2007; Kaya *et al.*, 2008; Paris *et al.*, 2002; Li *et al.*, 2014).

In addition to S1P, C1P may be another bioactive sphingolipid capable of modulating vascular development and apoptosis in ovaries affected by chemotherapy. C1P is produced by ceramide kinase (CerK) and can act both intracellularly and through a putative membrane receptor to exert its biological effects (Gomez-Munoz *et al.*, 2013). C1P regulates different cellular processes including cell proliferation, cell migration, angiogenesis, calcium mobilization and apoptosis (Gómez Muñoz *et al.*, 2004; Gangoiti *et al.*, 2011; Arana *et al.*, 2013; Niwa *et al.*, 2009).

Unlike S1P, C1P is metabolized slowly and is more stable in biological fluids. For these reasons, C1P possesses a longer half-life than S1P (Gomez-Munoz *et al.*, 1995; Gangoiti *et al.*, 2012). Since C1P is a potent sphingolipid released by damaged tissue cells (Kim *et al.*, 2013), it could emerge as a novel mediator in the repair of damaged organs and tissues. This makes C1P another candidate for therapy in patients who undergo chemotherapy and/or irradiation, promoting ovarian angiogenesis and inhibiting follicular atresia.

So far, no studies have evaluated the involvement of C1P in ovarian pathological conditions such as chemotherapy-induced POF. Therefore, the main objective of this study was to evaluate the effects of *in-vivo* intrabursal C1P administration on follicular development, ovarian reserve, apoptosis, vascular development and stability in ovaries and also on uterine morphology in a chemotherapy-induced mice model. Additionally, we analysed fertility parameters in this model.

Materials and Methods

C1P (#860532P) was purchased from Avanti Polar Lipids (Alabaster, AL, USA) Cyclophosphamide (CAS no. 6055-19-2) was from Sigma-Aldrich (St. Louis, MO, USA), as well as proteinase K, sodium dodecyl sulphate (SDS), NaCl, bovine serum albumin (BSA), methanol, Bradford reagent, Tris base, NP-40, glycerol and Tween-20. Hydrogen peroxide solution was from Merck Millipore (Darmstadt, Germany) and 3,3′-diaminobenzidine (DAB) was from Roche Applied Science (Mannheim, Germany). All other chemicals were of reagent grade and were obtained from standard commercial sources.

Ethical approval of animal use

All procedures were approved by the ethics committee of the IByME (Protocol CE-042-6/2015) and conducted according to the guide for the care and use of laboratory animals of the National Institute of Health (USA).

Animal model and experimental design

First filial generation hybrid mice of a cross between C57BL/6 male × Balb/c female mice were housed under pathogen-free conditions and cared at the Instituto de Biología y Medicina Experimental (IByME), Buenos Aires, Argentina. The mice from our colonies were maintained on a continuous cycle of lights on at 7 a.m. and off at 7 p.m., with food and water available ad libitum. The room temperature was maintained at 21–23°C.

The 6–8-week-old mice were weighed and administered either a single intraperitoneal injection of Cy (75 mg/kg, 200–300 µl) or an equal volume of saline solution only for control mice. All experimental groups were anesthetized with ketamine HCl (70 mg/kg; Holliday-Scott S.A., Buenos Aires, Argentina) and xylazine (5 mg/kg; König Laboratories, Buenos Aires, Argentina) and the ovaries were exteriorized through an incision made in the dorsal lumbar region. Control and Cy mice underwent sham surgery and received an intrabursal injection of saline solution, while Cy + C1P animal groups received either 5 µl C1P 0.5 or 1 mM under the bursa of both ovaries, 1 h prior to Cy administration. For preliminary experiments, both doses were assessed. Based on those results, the dose of 1 mM was chosen for subsequent assays.

Except for the mice that were kept alive for fertility assessments, animals were euthanized 2 weeks after surgery and treatment administration. Mice were euthanized by cervical dislocation either for ovary and uterus collection or for oocyte recovery followed by IVF assays. Collected organs were cleaned of adhering tissue in culture medium and used for subsequent assays (Western blotting, histological analysis and/or histochemical techniques). The set of animals destined for hormone measurements was anesthetized and sacrificed by terminal cardiac puncture, and their ovaries were stored for steroid extraction.

Histological processing and follicle count

Ovaries and uterine horns were extracted and immediately fixed in Bouin solution for 12 h. For H&E staining, paraffin-embedded organs were cut into 5-µm histological sections and serial sections were mounted on slides. After deparaffinization and rehydration, a set of uterine sections was stained with H&E and examined under the light microscope by an experienced gynaecologic pathologist, who was blinded to the group assignment.

As for ovarian morphology, follicles were classified and counted to assess the effect of the chemotherapy on ovarian follicles and to evaluate protective effects of C1P. All follicle counts were performed by two independent researchers, blinded to the experimental groups, as described by Kalich-Philosoph *et al.* (2013) with minor modifications. Briefly, ovaries were serially sectioned every 5 µm and every fifth section was stained with H&E. Only those follicles in which the nucleus of the oocyte was clearly visible were scored. A follicle was counted as primordial when it contained an intact oocyte surrounded by a single layer of flattened squamous follicular cells. A primary follicle was defined as an enlarged oocyte surrounded by a single layer of cuboidal granulosa cells. Oocytes with two or more layers of granulosa cells but no visible space between granulosa cells were identified as preantral follicles. Antral follicles were scored when containing several layers of granulosa cells, an oocyte with a clear nucleus, an antrum and a theca layer. Atretic follicles were counted only when a degenerating oocyte and pycnotic granulosa cells were observed. The number of follicles in each stage was estimated by counting every fifth section and multiplying the final sum by a correction factor of 5, to represent the whole ovary (Tilly, 2003). Data are presented as number of follicles per developmental stage ($n = 8$ ovaries per group).

To corroborate the correct count of primordial follicles, an IHC was also performed and DDX4-positive follicles were counted. DDX4, also known as VASA, belongs to the protein family of an ATP-dependent RNA helicase of the DEAD (Asp-Glu-Ala-Asp)-box (Fujiwara *et al.*, 1994). DDX4 is a germ cell-specific marker considered to be expressed and localized in plasma membrane of putative germ stem cells of postnatal ovaries.

Histochemistry and immunohistochemistry in ovarian tissues

For IHC, 5-µm tissue sections were deparaffinized in xylene and rehydrated by graduated ethanol washes. Endogenous peroxidase activity was inactivated by 3% (vol/vol) hydrogen peroxide in PBS and non-specific binding was blocked with 2% BSA 1 h, at RT°. Sections were incubated with primary antibody or biotinylated lectin BS-1 (from Bandeiraea simplicifolia, 20 mg/ml) overnight at 4°C. The antibodies used were anti-DDX4

(1:100, ab27591, Abcam, Cambridge, MA, USA), AMH (1:400, sc-6886, Santa Cruz Biotechnology, Inc., Santa Cruz, CA, USA) anti-Von Willebrand factor (vWF) (1:100, A0082, Dako, Glostrup, Denmark) and anti- α-SMA (1:250, ab18147, Abcam). Lectin BS-1 is a constitutive endothelial cell marker for many tissues, including the ovary (Augustin *et al.*, 1995; Redmer *et al.*, 2001; Cherry *et al.*, 2008; Scotti *et al.*, 2014). After washing, slides were incubated with biotinylated anti-mouse or anti-rabbit IgG for 1 h (except in the case of lectin BS-1) and afterwards with avidin-biotinylated horseradish peroxidase Complex for 30 min (BA-9200, BA-1000 and Vectastain ABC system, respectively, from Vector Laboratories, Burlingame, CA, USA). Finally, protein signal was visualized with DAB staining. After stopping the reaction with distilled water, slides were counterstained with haematoxylin, dehydrated and mounted (Canada Balsam Synthetic, Biopack, Argentina). For AMH slides, no counterstaining was performed to better visualize labelled follicles. In all cases, negative controls were obtained in absence of primary antibody or lectin.

The images were taken with a digital camera (Nikon, Melville, NY, USA) mounted on a conventional light microscope (Nikon), using a magnification of ×40. Three sections per ovary were studied (six ovaries/group) and at least five fields were photographed and analysed per each section.

Western blot

Ovaries were removed, placed on ice and resuspended in five volumes of lysis buffer (20 mM Tris–HCl pH 8, 137 mM NaCl, 1% Nonidet P-40 and 10% glycerol) supplemented with protease inhibitors (0.5 mM PMSF, 0.025 mM N-CBZ-L-phenylalanine chloromethyl ketone, 0.025 mM N-p-tosyl-lysine chloromethyl ketone and 0.025 mM L-1-tosylamide-2-phenyl-ethylchloromethyl ketone) and homogenized with an Ultra-Turrax homogenizer (IKA Werk, Breisgau, Germany). Samples were centrifuged at 4°C for 10 min at 10 000 *g* and the resulting pellets were discarded. Protein concentration in the supernatant was measured by the Bradford assay. After boiling for 5 min, 40 µg of protein was applied to a 12% SDS-polyacrylamide gel and electrophoresis was performed at 150 V for 1.5 h. The resolved proteins were transferred onto nitrocellulose membranes at 80 V for 2 h. The blot was then incubated in blocking buffer (5% non-fat milk, 0.05% tween-20 in 20 mM TBS pH 8.0) for 1 h at room temperature and incubated overnight at 4°C with appropriate primary antibodies: BAX (1:300, sc-493, Santa Cruz Biotech.), BCLX-L (1:100, sc-634, Santa Cruz Biotech), AMH (1:400, sc-6886, Santa Cruz Biotechnology, Inc., Santa Cruz, CA, USA) and A-SMase (1:200, ab83354, Abcam). The blot was then incubated with anti-rabbit secondary antibodies conjugated with horseradish peroxidase (1:1000, A4914, Sigma Aldrich) and signal was detected by chemiluminescence. The protein levels were analysed by densitometry using Scion Image for Windows (Scion Corporation, Worman's Mill, CT, USA). Optical density data are expressed as arbitrary densitometric units ± SEM.

Steroid extraction from ovarian tissue

Steroids were extracted from ovaries as previously described (Pascuali *et al.*, 2015). Whole ovaries were mechanically homogenized in acetone (1:10 weight/volume) with an Ultra-Turrax homogenizer (IKAWerk, Breisgau, Germany). Labelled steroids were added as internal standards, with a recovery percentage between 60 and 80%. After 10-min centrifugation (1600 *g*), supernatants were collected and transferred to conical tubes and evaporated to dryness. Next, 1 ml of distilled water was added to each tube and samples were extracted twice with diethyl ether (1:2.5 vol/vol). Each time, ether fractions were separated by freezing the samples at −70°C for 20 min and then transferring the liquid phases to new tubes and evaporating to dryness. The remaining residue was dissolved in 1.4 ml of methanol. After adding 1.4 ml of distilled water to each tube, the samples were subjected to solvent partition with *n*-hexane. The upper layer was discarded and 2 ml of dichloromethane was added to the lower phase. After mixing for 2 min, the aqueous upper phase was discarded while the lower phase was evaporated to dryness. Finally, residues were resuspended in RIA buffer (Na_2HPO_4 40 mM; NaH_2PO_4 39.5 mM, NaCl 155 mM, sodium azide 0.1%, gelatin 1%, pH = 7.0) and stored at −20°C until further analysis.

Hormone measurements

Serum FSH and ovarian estradiol (E2) levels were measured by radioimmunoassay (RIA) (n = 6/group), as previously described (Irusta *et al.*, 2007; Di Giorgio *et al.*, 2013). Briefly, blood was collected by cardiac puncture and left to clot at room temperature for 45 min. Serum was obtained following centrifugation at 3000 *g* and stored at −20°C until further analysis. FSH protein concentration was determined by RIA with kits from NHPP, NIDDK & Dr. Parlow. Results were expressed in terms of RP3 rat FSH standards, as these systems recognize mouse samples. The assay sensitivity for FSH was 0.1175 ng/ml. Intra- and inter-assay coefficients of variation forFSH were 8.0 and 13.2%, respectively. The values are expressed as ng per ml of serum. E2 concentration in ovarian tissue was measured using a specific antibody supplied by Dr G.D. Niswender (Animal Reproduction and Biotechnology Laboratory, Colorado State University, Fort Collins, CO, USA). Under these conditions, the intra-assay and inter-assay variations were 7.2 and 12.5% for E2. The values are expressed as ng per mg of ovarian protein.

TUNEL assays

For quantification of apoptosis, tissue sections previously fixed in Bouin solution were processed for in situ localization of nuclei exhibiting DNA fragmentation by the TUNEL technique (D'Herde *et al.*, 1994) with an apoptosis detection kit (Apoptag plus peroxidase *in situ* Apoptosis detection kit; Chemicon International, Inc., Temecula, CA) as previously described (Andreu *et al.*, 1998; Scotti *et al.*, 2011). The 5-µm thick tissue sections were deparaffinized and digested for 15 min at room temperature with proteinase K. Endogenous peroxidase was quenched with 3% hydrogen peroxide in PBS. The labelling reaction was carried out by incubating tissue sections with buffer containing digoxygenin-20-deoxyuridine 50-triphosphate prior to incubation with terminal deoxynucleotidyl transferase (TdT) for 1 h at room temperature. Tissues were then incubated for 30 min with a peroxidase-conjugated antidigoxygenin monoclonal antibody, and apoptotic cells were visualized as positively immunostained structures after reaction with diaminobenzidine. Negative controls included TdT omission. Sections were counterstained with methyl green. The number of apoptotic cells was determined by counting labelled cells from all follicle types in ×400 microscopic fields (four sections per ovary; five ovaries per group). Follicles presenting more than 5% labelled cells were considered unhealthy. The apoptotic index was calculated as a fraction of unhealthy/total follicles for each class.

Fertility assessment

Two breeding rounds were performed to assess the effect of Cy chemotherapy on litter production, as well as the potential protective effects of C1P. The 8-week-old female mice were divided into three groups (n = 5–6 mice per group) and treated with a non-sterilizing dose of 75 mg/kg Cy, with or without C1P coadministration (1 mM). To ensure two full cycles of primordial follicle activation following treatment administration, mating trials started 8 weeks post-treatment. Female mice were housed with untreated adult C57 males of proven fertility at a 1:1 ratio. Mice were examined every morning for mating evidence (presence of vaginal plug). On the day when copulation was confirmed, females were removed to a separate cage and housed individually until the delivery of the pups. Gestation length and offspring data (number of pups per litter and pup weight at postnatal Day 2) were recorded. The second breeding round

started 12 weeks after treatment. Males were randomly rotated for each breeding round.

Oocyte collection and IVF and embryo development assays

IVF was performed as previously described (Gomez-Elias *et al.*, 2016). Briefly, three female mice per treatment were superovulated by an injection (i.p.) of equine chorionic gonadotrophin (eCG; 5UI; Syntex, Argentina) 1 h before the lights turned out, followed by the administration (i.p.) of hCG (5 UI) 48 h later. Oocyte–cumulus complexes were collected from the oviducts 13–14 h after hCG administration. Cumulus-intact oocytes were inseminated with capacitated spermatozoa (final concentration: 5–6 × 10^5 spermatozoa/ml) and gametes were co-incubated for 3 h at 37°C in an atmosphere of 5% (*v*/*v*) CO_2 in air. Oocytes were then classified as normal or abnormal (dead or fragmented). Normal oocytes were transferred to fresh medium, and 15 h later the number of two-cell embryos was recorded.

Two-cell embryos were transferred to 50 ml drops of fresh KSOM medium at 37°C in a 5% (*v*/*v*) CO_2 atmosphere in air, and incubated for 4 days and the developmental stage of each embryo was determined in an inverted microscope (Nikon Eclipse TS100, Nikon).

Statistical data analyses

The results are expressed as the mean ± SEM. The significant differences between groups were determined using ANOVA, followed by Tukey's test in all cases (except for evaluation of fertility index, where chi-square analysis was performed). All samples were tested for normality before ANOVA. *P* values < 0.05 were considered statistically significant. Different letters indicate statistically significant differences between groups; means that share the same letter do not differ significantly. Data were statistically analysed using GraphPad Prism 6.0.

Results

Effect of C1P on ovarian folliculogenesis in the Cy-induced gonadotoxicity model

As evidenced by histological assessment, Cy-treated ovaries are damaged and poor in follicles in comparison to control ones, as they present cortical fibrosis and altered stromal cells, while both Cy + C1P groups are similar to healthy, control ovaries (Fig. 1).

The number of primordial ($P < 0.01$), primary ($P < 0.05$) and preantral follicles ($P < 0.05$) were decreased in Cy-treated mice (Fig. 1A) compared to control animals, while atretic follicles were increased ($P < 0.001$), which further shows the chemotoxic effect of Cy. When C1P is given in combination with Cy, the ovaries recover control numbers of these follicular structures in both C1P doses studied (primordial follicles: $P < 0.05$ and $P < 0.01$; primary follicles: $P < 0.05$ and $P < 0.01$; preantral follicles: $P < 0.01$ and $P < 0.001$; atretic follicles: $P < 0.05$ and $P < 0.01$; Cy vs Cy + Cy C1P 0.5 mM and 1 mM, respectively). Moreover, the total sum of all follicle stages is significantly lower in Cy-treated mice compared to control ones ($P < 0.05$). While the follicle sum in the Cy + C1P 0.5 mM group remained similar to control mice (but no different than Cy-treated mice), C1P at a higher dose (1 mM) was able to prevent the overall decrease observed in the Cy group ($P < 0.01$). Given that complete recovery of the number of different follicle stages was achieved with the 1 mM dose, this concentration was chosen for all subsequent experiments.

Effect of C1P on ovarian expression of AMH in the Cy-induced gonadotoxicity model

As expected, AMH expression was found in granulosa cells of primary to early antral follicles, since it is no longer expressed during the FSH-dependent final stages of follicle growth and disappears when follicles become atretic. The results of the IHC revealed that Cy severely affects AMH expression, while the expression of AMH was at least partially recovered when C1P is administered as well (Fig. 2A). These results were corroborated by Western blot for AMH (Fig. 2B). We observed that Cy decreased AMH expression compared to control animals ($P < 0.05$), whilst it increased with C1P-cotreatment to levels no different than those of control animals ($P > 0.05$ vs control and Cy groups).

Effect of C1P on steroid hormones in the Cy-induced gonadotoxicity model

To evaluate the effect of C1P on steroid hormone levels, serum FSH and ovarian tissue estradiol (E2) were measured by RIA and compared among the experimental groups (Fig. 3). Treatment with Cy caused an increase in serum FSH concentration ($P < 0.01$), which was prevented by C1P coadministration ($P < 0.01$, Cy vs Cy + C1P). E2 was decreased significantly in Cy-treated ovaries compared to controls ($P < 0.01$), whilst C1P restored E2 to levels no different from that in control ovaries ($P > 0.05$, vs control and Cy groups).

Effect of C1P on apoptosis in the Cy-induced gonadotoxicity model

Expression of proapoptotic BAX and antiapoptotic BCLX-L is presented in Fig. 4. Cy treatment increased the expression of BAX ($P < 0.01$) and decreased the expression of BCLX-L compared to control ovaries ($P < 0.01$). Ovarian BCLX-L:BAX ratio was also lower in Cy-treated mice ($P < 0.05$). When C1P was administered in combination with Cy, expression levels of BAX, BCLX-L and BCLX-L:BAX ratio were restored to those in control ovaries (Fig. 4A–C). In Cy + C1P mice, BAX expression was lower ($P < 0.01$) and BCLX-L expression was higher ($P < 0.05$) compared to Cy-treated animals. In addition, acid sphingomyelinase (A-SMase), an enzyme known to increase the levels of the proapoptotic sphingolipid ceramide, presented higher expression levels in Cy-treated ovaries compared to control ($P < 0.05$), whilst levels in the Cy + C1P group were partially protected (no different from control or Cy mice; $P > 0.05$) (Fig. 4D).

Cleaved caspase-3 IHC and TUNEL reaction were then carried out to identify apoptotic cells. We observed an abundance of growing follicles (preantral to mature antral follicles) with extensive granulosa cell apoptosis in Cy mice, but it was not as severe in ovaries cotreated with C1P, as shown in Fig. 5A. Based on TUNEL sections, all follicles were classified according to their developmental stage and labelled cells were quantified (Fig. 5B). The results show that Cy treatment increased the apoptotic index (TUNEL-positive follicles/total follicles) in preantral and early antral stages, compared to control ovaries ($P < 0.001$ and $P < 0.01$, respectively). C1P protected follicles from this increase, since the apoptotic indexes in the Cy + C1P group for those follicular stages were

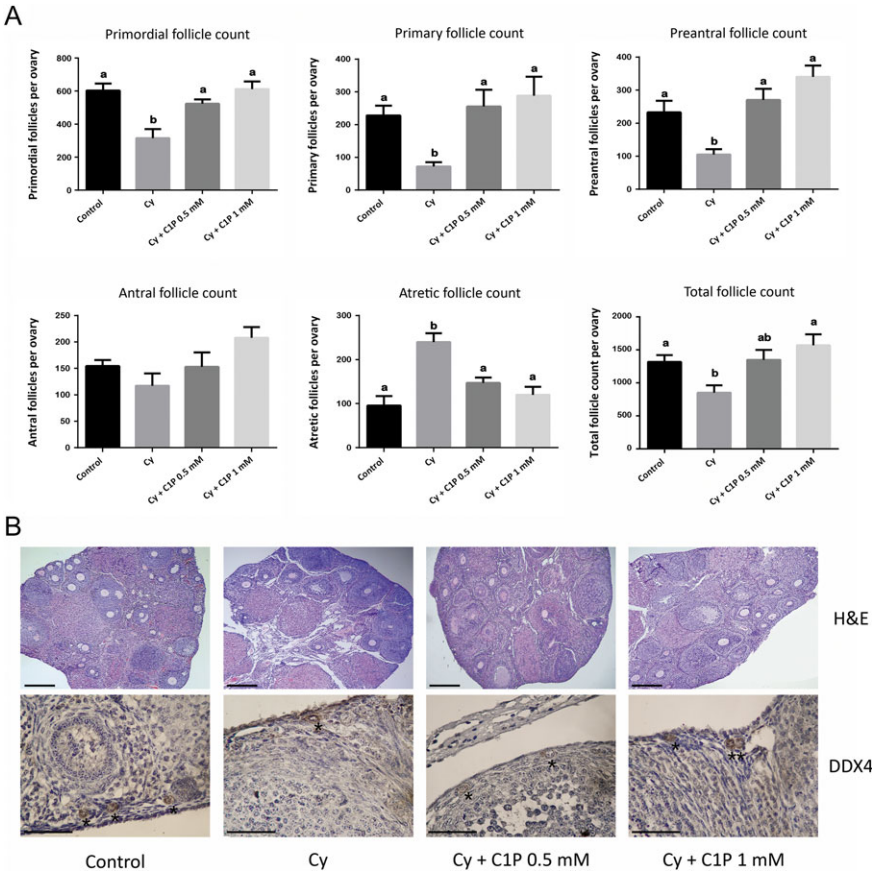

Figure 1 Ceramide-1-phosphate (C1P) administration prevents the loss of different follicle types and decreases atresia caused by cyclophosphamide (Cy) treatment. (**A**) Effect of Cy and Cy + C1P coadministration on the number of primordial, primary, preantral, antral, atretic follicles and on total follicles after 2 weeks of treatment (n = 6–8/group). Data are expressed as the mean ± SEM. Statistical analyses were performed by one-way ANOVA followed by Tukey's multiple-comparison test. Different letters represent statistically significant differences between groups (a vs b: P < 0.01–0.05), whereas means that share the same letter do not differ significantly. (**B**) Representative images of H&E and DDX4-immunostained ovarian histological sections from all experimental groups. Upper panel: Photomicrographs of H&E stained sections from control, Cy and Cy + C1P mice. Scale bars represent 200 μm. Lower panel: Germ cell staining with anti-DDX4 IHC for primordial follicle identification. Asterisks indicate primordial follicles. Scale bars represent 50 μm.

significantly lower and similar to controls (preantral: $P < 0.001$ and early antral: $P < 0.05$, Cy vs Cy + C1P). There were no primordial or primary follicular cells stained for either cleaved caspase-3 or TUNEL when exposed to Cy, therefore, we have found no evidence for the follicular reserve depletion in response to Cy being due to apoptosis.

Effect of C1P on ovarian vasculature in the Cy-induced gonadotoxicity model

Control sections show a homogeneous and hypercellular ovarian stroma that comprises most of the ovarian tissue, with no clear limits between cortex and medulla. As shown in Fig. 6, several blood vessels are distributed among the follicles. The endothelial layer is continuous, as evidenced by IHQ with vWF and lectin staining.

Treatment with Cy caused thickening and hyalinization of the vascular wall, at the expense of vessel lumen; this finding was especially clear in large cortical stromal structures. Furthermore, there were sectors of discontinuation of the endothelial layer, suggesting a certain grade of vascular injury. Probably in response to this damage, Cy-treated ovaries also exhibited an increase in small, newly formed vessels (neovascularization), localized predominantly near follicles.

Interestingly, the thickening of vascular walls was less pronounced in the Cy + C1P ovaries, and nearly no neovascularization was seen. Moreover, the number of stromal vascular structures seemed to be restored and the continuity of the endothelial layer was almost totally recovered, which suggests at least a partial protection from Cy-induced damage (Fig. 6A and B).

α-SMA immunostaining allows for the visualization of peri-endothelial cells such as pericytes and vascular smooth-muscle cells (Fig. 6C). In control conditions, α-SMA-positive cells were frequently observed in stromal and in follicle-associated vessels at the perivascular area. In contrast, in Cy-treated ovaries, α-SMA-positive cells were detected in a disrupted distribution around blood vessels, suggesting a poor pericyte coverage and thus a lower vascular maturity. Consistent

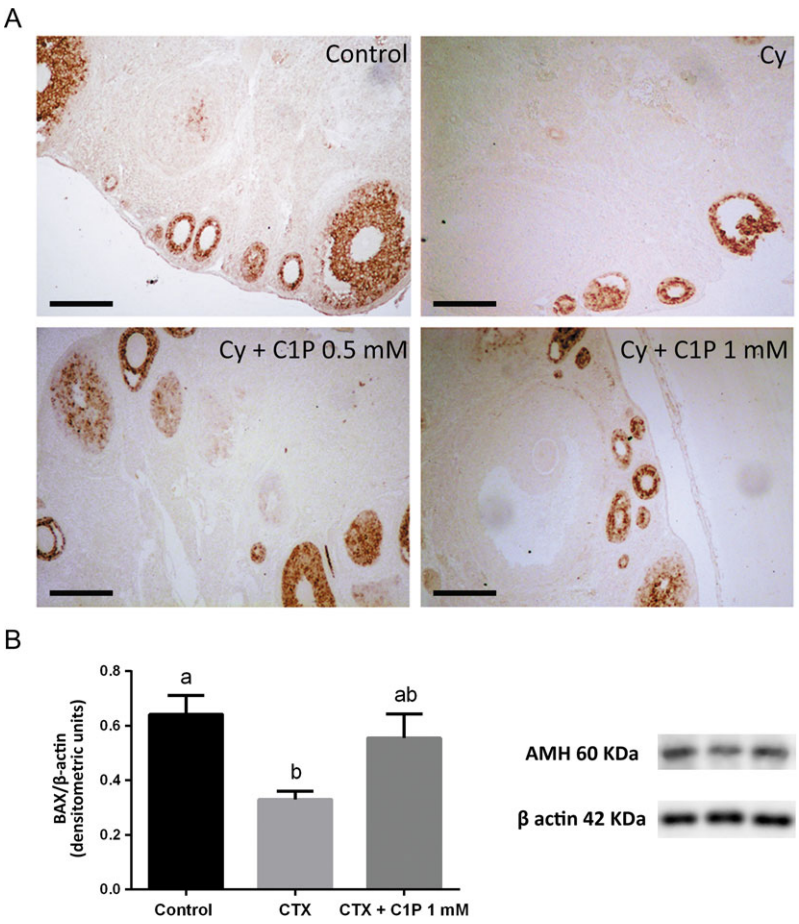

Figure 2 Ceramide-1-phosphate (C1P) increases anti-Müllerian hormone (AMH) expression in cyclophosphamide (Cy)-treated ovaries. (**A**) Representative photomicrographs of AMH immunostaining in mice ovaries, for all experimental groups (control, Cy and both Cy + C1P doses). Brown-yellow colouring of cell cytoplasm was considered as positive staining. Scale bars represent 100 μm. (**B**) AMH protein expression in ovaries as analysed by Western blot, including quantification of AMH relativized to β-actin (left) and a representative blot of each protein (right). CTX = Cy. Data are expressed as the mean ± SEM of three independent experiments. Statistical analysis was performed by one-way ANOVA followed by Tukey's multiple-comparison test. Different letters represent statistically significant differences between groups (a vs b: $P < 0.05$), whereas means that share the same letter do not differ significantly.

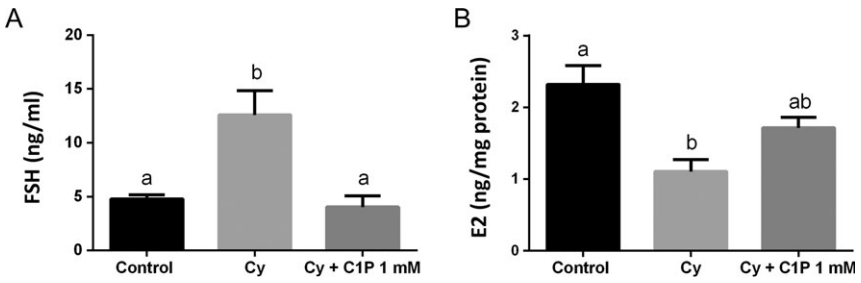

Figure 3 Ceramide-1-phosphate (C1P) normalizes FSH and E2 concentrations in cyclophosphamide (Cy)-treated mice. (**A**) Serum concentration of FSH in control, Cy and Cy + C1P animals, as assessed by radioimmunoassay (RIA). Data are expressed as FSH ng/ml of serum. (**B**) E2 concentration in ovaries from control, Cy and Cy + C1P mice. Values are relative to ovarian protein content and are expressed as E2 ng/mg of protein. Statistical analyses were performed by one-way ANOVA followed by Tukey's multiple-comparison test. Different letters represent statistically significant differences between groups (a vs b: $P < 0.01$), whereas means that share the same letter do not differ significantly.

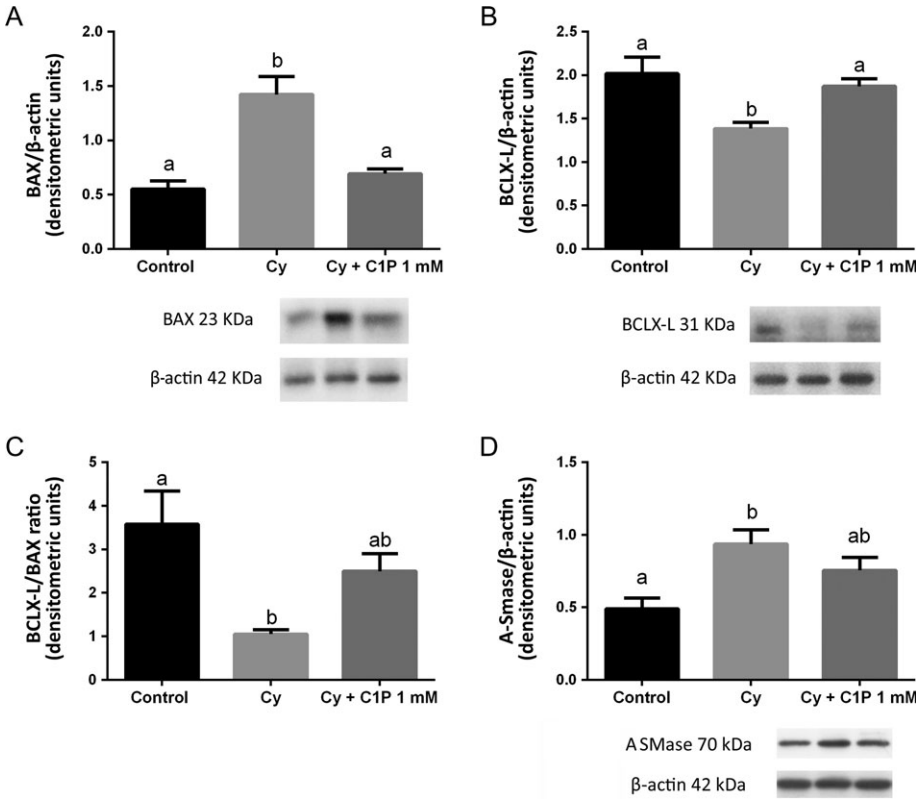

Figure 4 Ceramide-1-phosphate (C1P) modulates ovarian expression of pro- and antiapoptotic proteins in cyclophosphamide (Cy)-treated mice. A series of Western blot analyses from control, Cy and Cy + C1P 1 mM groups show expression of BAX, BCLX-L, A-SMase and β-actin, as indicated. Bar graphs show the respective densitometric quantification for each protein or protein ratio in the experimental groups ($n = 5$). (**A**) Densitometric analysis of BAX expression. (**B**) Densitometric analysis of BCLX-L expression. (**C**) Densitometric analysis of BCLX-L/BAX ratio. (**D**) Densitometric analysis of A-SMase expression. In all cases, data are expressed as the mean ± SEM of three independent experiments and a representative blot of each protein is shown. Statistical analyses were performed by one-way ANOVA followed by Tukey's multiple-comparison test. Different letters represent statistically significant differences between groups (a vs b: $P < 0.01$–0.05), whereas means that share the same letter do not differ significantly.

with vWF and lectin results, C1P coadministration prevented the Cy-induced effects, at least partially, with a higher proportion of α-SMA-positive cells surrounding vascular structures, leading to greater vascular stability.

Effect of C1P on uterine morphology in the Cy-induced gonadotoxicity model

H&E stained sections of uterus from control, Cy, Cy + C1P in both doses (0.5 and 1 mM) were assessed in a comparative manner (Fig. 7). Under control conditions, uterine horns and fundus consisted of an inner epithelial-lined mucosa (endometrium), covering the muscular layer of the uterus (myometrium). The endometrium was arranged in elevated transverse folds supplied by blood vessels and nerves. The mucosal epithelium was composed of simple columnar cells extending into branched tubular glands within the endometrial stroma, which consists of loosely arranged reticular connective tissue and many polyhedral cells. Cy-treated mice presented endometrial alterations compared to control, affecting both epithelial and stromal compartments. We observed a severe decrease in the number of glandular branches as well as in the amount of stroma, at the expense of the original loose connective tissue. By contrast, when C1P is combined with Cy at either dose, the stromal tissue maintained its loose quality and its glandular branches. Additionally, there was an increase in vascular structures, predominantly in the endometrium and in the stratum vasculosum.

Effect of C1P on fertility parameters in the Cy-induced gonadotoxicity model

To assess the protective effect of C1P on fertility parameters, *in-vivo* mating trials were performed. Table I summarizes the fertility parameters studied. Mating was confirmed in all females in both breeding rounds, as judged by the presence of vaginal plugs in all cases 1–3 days after being housed with males.

Although no differences were observed in measured parameters in the first breeding round, only two out of five Cy-treated female mice produced litters in the second round, while all females were fertile in both the control and Cy + C1P groups (Table I, $P = 0.0133$). In addition, Cy-treated animals that did become pregnant had reduced numbers of pups per litter compared to the controls (Table I, $P < 0.05$). Interestingly, Cy + C1P mice produced more pups per litter compared

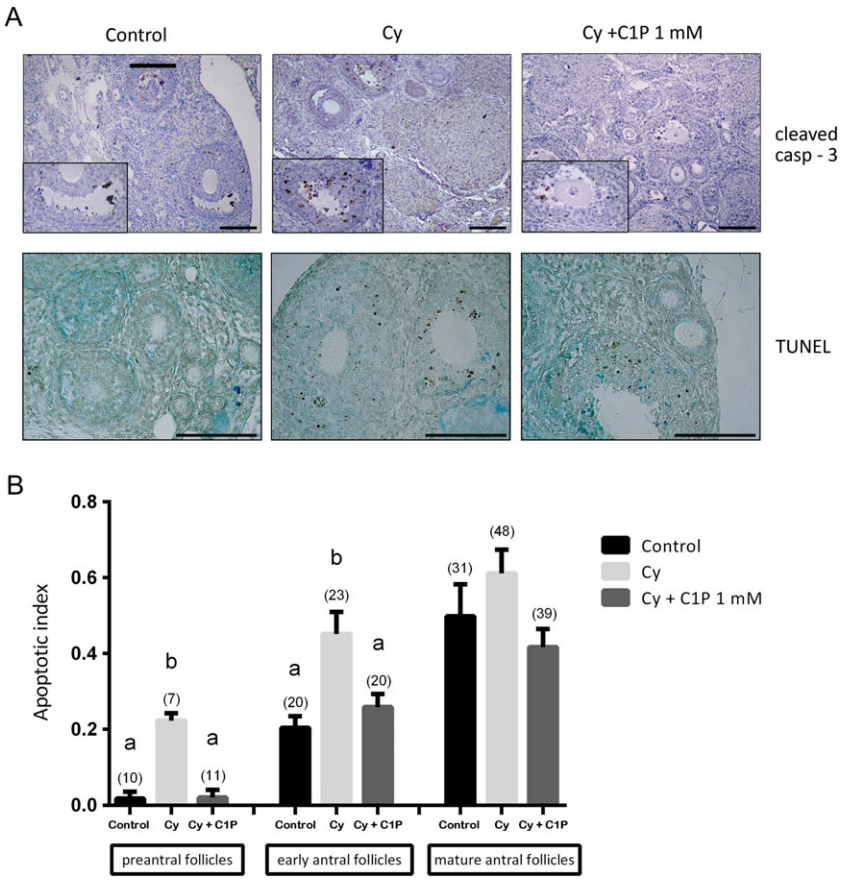

Figure 5 Ceramide-1-phosphate (C1P) coadministration decreases cyclophosphamide (Cy)-induced apoptosis in mouse ovarian follicles. (**A**) Microphotographs of mouse ovaries stained with cleaved caspase-3 antibody (upper panel) and TUNEL (lower panel). Bars represent 100 μm. Representative images are shown for each treatment condition. Insets are digital magnifications. (**B**) TUNEL-based quantification of the apoptotic index per follicle class calculated as fraction apoptotic/total follicles for each type. $n = 5$ mice, a vs b: $P < 0.001$–0.01, one-way ANOVA, Tukey test comparison. The numbers in between brackets represent the average number of TUNEL-positive cells present for each follicle type and treatment condition. Primordial and primary follicles did not present TUNEL-positive cells in any experimental group. Statistical analyses were performed by one-way ANOVA followed by Tukey's multiple-comparison test. Different letters represent statistically significant differences between groups (a vs b: $P < 0.01$–0.05), whereas means that share the same letter do not differ significantly.

to Cy-treated mice, though the results did not reach significance ($P > 0.05$) when compared to either control or Cy-treated mice.

Effect of C1P on oocyte quality and IVF in the Cy-induced gonadotoxicity model

To evaluate whether the effect of treatment on female fertility was due to alterations on oocyte quality, we performed IVF experiments with oocytes recovered from superovulated females treated with Cy, either alone or in combination with intrabursal injection of C1P. The total number of recovered oocytes was similar among experimental groups (data not shown). Nevertheless, Cy treatment resulted in a significantly higher proportion of abnormal oocytes compared to control ($P < 0.05$) and this was prevented by C1P administration ($P < 0.05$), as shown in Fig. 8.

Normal oocytes were further incubated to evaluate fertilization ability. None of the treatments altered the percentages of oocytes that developed to two-cell embryo stage (control: 77.6 ± 11.4, Cy: 81.6 ± 10.2, Cy + C1P: 79.4 ± 6.5). Additionally, to determine whether Cy hinders preimplantation embryo development, progression of development of the two-cell embryos was monitored. No significant differences in the percentage of blastocysts were found among the experimental groups (control: 91.0 ± 9.0, Cy: 81.7 ± 3.2, Cy + C1P: 75.8 ± 10.2).

Discussion

The common side effects associated with chemotherapy in female survivors include ovarian damage, early menopause and infertility (Blumenfeld *et al.*, 1999; Falcone and Bedaiwy, 2005; Meirow and Nugent, 2001).

In our study, we used the alkylating agent Cy. Cy, a commonly used chemotherapeutic agent in antitumoral therapies, induces intra- and inter-strand DNA cross-linking, affecting cellular division (Stefansdottir *et al.*, 2014). In particular, Cy causes severe ovarian damage including altered folliculogenesis and steroid production, destruction of growing

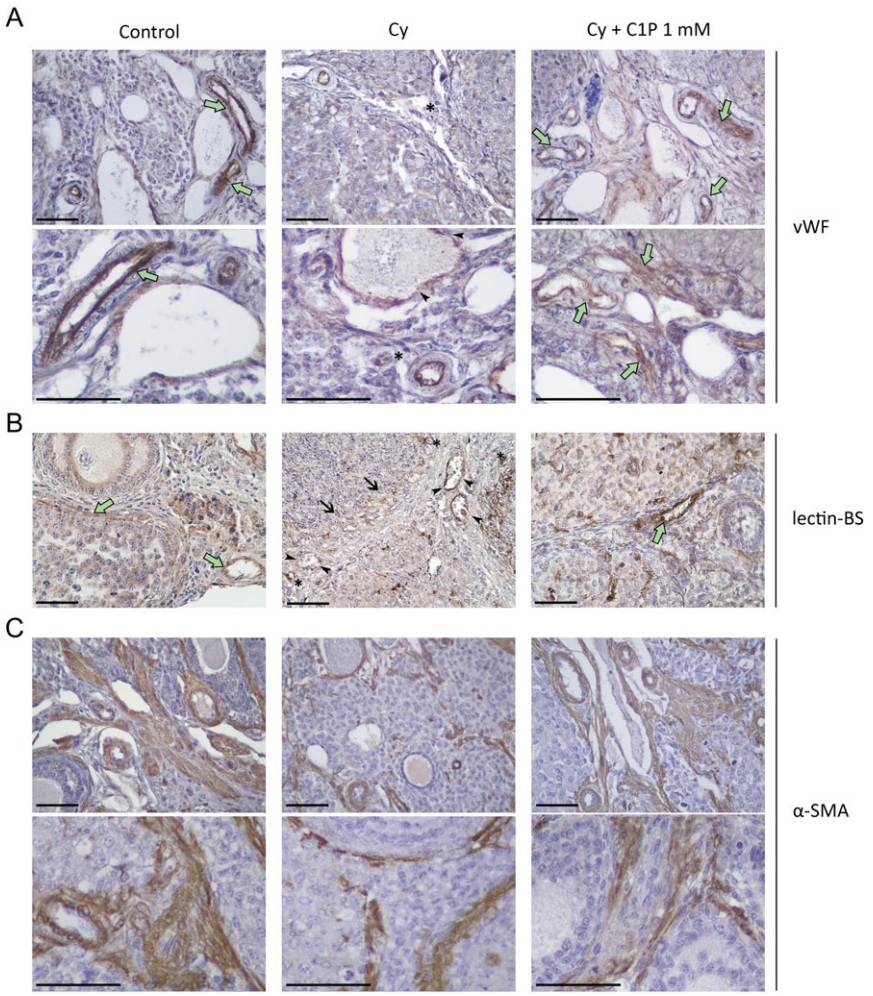

Figure 6 Ceramide-1-phosphate (C1P) protects ovarian vessels from cyclophosphamide (Cy)-induced damage. Representative microphotographs of endothelial staining with vWF (**A**) and lectin-BS (**B**) and of peri-endothelial cell staining with α-SMA (**C**) in ovaries from control (left), Cy (middle) and Cy + C1P 1 mM mice (right). Note the disruptions in stromal vasculature (arrowheads), the sparse and intermittent staining in thecal vasculature (black arrows) and the small vessels characteristic of neovascularization (asterisks) in Cy ovaries, in comparison with the broad, continuous bands of staining (green arrows) in control and Cy + C1P ovaries. Scale bars represent 50 μm.

follicles and thereby reduced follicle numbers (Jarrell *et al.*, 1987; Kalich-Philosoph *et al.*, 2013; Plowchalk *et al.*, 1992)

The current strategies to protect the ovary from chemotherapy do not ensure a safeguard for female fertility. In the present study, we evaluated the sphingolipid C1P as a cytoprotective factor from Cy toxicity in order to improve ovarian preservation. We demonstrated for the first time that intrabursal administration of C1P enhances folliculogenesis, increases estradiol levels and AMH protein expression, attenuates the loss of primordial follicles and decreases FSH levels and apoptosis, in ovaries from Cy-treated mice model. Additionally, we observed that local administration of this bioactive sphingolipid decreases stromal cell damage and disruption of blood vessels caused by chemotherapy. Additionally, C1P improved uterine morphology and fertility parameters in the above-mentioned model.

It is known that Cy causes a decrease in primordial follicles and primary follicles in ovaries from mouse and rat models (Desmeules and Devine, 2006; Petrillo *et al.*, 2011). Additionally, Raz *et al.* (2002) and Abir *et al.* (2008) have observed that the treatment with Cy affects preantral follicles in vitro and in vivo (Raz *et al.*, 2002; Abir *et al.*, 2008). Our study is the first to show that *in-vivo* C1P administration in ovaries from Cy-treated mice reduces primordial follicle loss, increase the number of primary and preantral follicles and decreases the number of atretic follicles. These results suggest that C1P protects ovarian reserve and improves follicular development, mitigating the severe ovarian damage caused by Cy. In line with these observations, there is previous data by several authors who employed a different sphingolipid, S1P. Morita *et al.* (2000) have shown that *in-vivo* therapy with S1P could prevent radiation-induced POF (Morita *et al.*, 2000). Additionally, Hancke *et al.* (2007) have demonstrated that local administration of S1P (2 mM) protects follicles from dacarbazine-induced cell death (Hancke *et al.*, 2007). Regarding this last study, it is important to mention that in our experiments we used even lower concentrations of C1P (0.5–1 mM) compared to those used in the study conducted by Hancke *et al.*

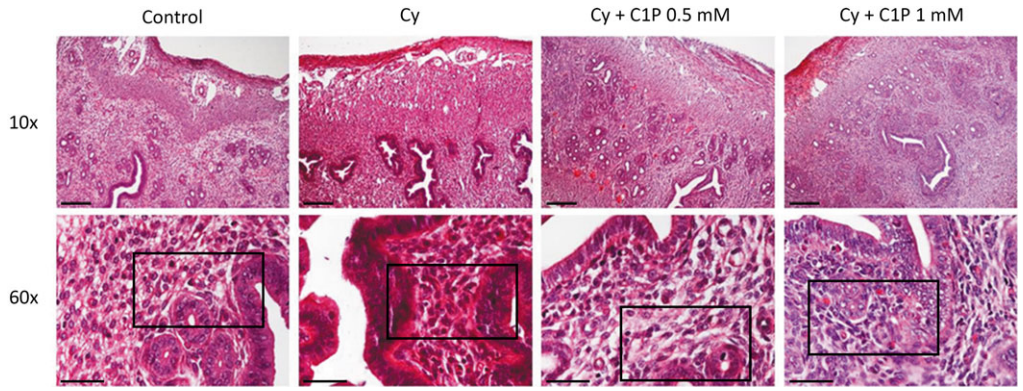

Figure 7 Ceramide-1-phosphate (C1P) prevents modifications in uterine morphology in cyclophosphamide (Cy)-treated mice. H&E stained sections show representative histological fields of control, Cy and Cy + C1P uterus (both doses). Cy uterine horns present alterations in both epithelial and stromal compartments when compared to control, while C1P administration helps maintain endometrial quality. The boxes indicate areas of stroma and glandular branches. Control and Cy + C1P groups exhibit normal loose stroma and numerous polyhedral cells, while these features are decreased in Cy-treated endometrium. Upper panels: original magnification 10×, bars represent 200 μm. Lower panels: original magnification 60×, bars represent 50 μm.

Table I Cyclophosphamide (Cy) reduces pregnancies and litter size in female mice, which is rescued by Ceramide-1-phosphate (C1P) administration.

	Round 1 (8 weeks after treatment)			Round 2 (12 weeks after treatment)		
	Control	Cy	Cy + C1P 1 mM	Control	Cy	Cy + C1P 1 mM
Mating index	5/5 (100%)	5/5 (100%)	6/6 (100%)	5/5 (100%)	5/5 (100%)	6/6 (100%)
Fertility index (fraction of females that delivered offspring/total)[†]	5/5 (100%)	4/5 (80%)	5/6 (83.3%)	5/5 (100%)[a]	2/5 (40%)[b]	6/6 (100%)[a]
Mean litter size (number of pups)[#]	9.8 ± 0.6	9.6 ± 1.3	8.2 ± 1.1	11.7 ± 1.2[a]	3.5 ± 1.5[b]	8.4 ± 1.5[ab]
Mean body weight of pups (g)[#]	1.52 ± 0.09	1.51 ± 0.03	1.64 ± 0.11	1.44 ± 0.07	1.52 ± 0.06	1.62 ± 0.12

Summary of fertility parameters for all the experimental groups (control, Cy and Cy + C1P) and times (8 and 12 weeks post-treatment). Different letters represent statistically significant differences between groups (a vs b: $P < 0.05$), whereas means that share the same letter do not differ significantly. [†]Statistical analysis was performed using Chi-square tests. [#]Statistical analyses were performed by one-way ANOVA followed by Tukey's multiple-comparison tests.

Primordial follicles represent the most important follicular population because this ovarian reserve is non-renewable. Activation of these follicles is irreversible and their growth ends with either ovulation or atresia. Accordingly, the quiescent ovarian reserve is crucial for the preservation of fertility. We showed that Cy diminished the primordial follicle population compared to the control, which is consistent with other studies (Desmeules and Devine, 2006; Oktem and Oktay, 2007). Nevertheless, C1P was able to reduce primordial follicle loss compared to untreated Cy-damaged ovaries. These results suggest that C1P could modulate different pathways which regulate primordial follicle population. It is known that the dormancy of this follicle stage is controlled by numerous factors such as PI3K/PTEN/akt signalling pathway, forkhead boxl2 (Foxl2), Foxo3a and AMH (Castrillon *et al.*, 2003; Durlinger *et al.*, 1999; Kalich-Philosoph *et al.*, 2013; Schmidt *et al.*, 2004). More studies are needed to elucidate the effect of C1P on these mechanisms that control activation of primordial follicles.

AMH is produced by granulosa cells from primary to early antral follicles and its main function is to inhibit activation of primordial follicles and to maintain the dormant ovarian reserve (Mitra *et al.*, 2007; La Marca *et al.*, 2009). Serum AMH levels represent a predictor factor of the growing follicle population and correlates with the number of primordial follicles (Marcello *et al.*, 1990). Indeed, the measurement of AMH levels has been evaluated as a possible marker of ovarian function after treatment for women with breast cancer (Anderson and Cameron, 2011). In our study, we showed that ovarian expression of AMH was reduced in Cy-treated ovaries compared to the control group. This result is consistent with previous data observed by Rosendahl *et al.* (2010), who showed that AMH levels are lower during chemotherapy. In the present study, we also demonstrated that C1P increased the expression of AMH in ovaries from Cy-treated mice. One possible explanation would be that C1P may prevent the ovarian damage caused by Cy treatment by inducing the expression of AMH and, consequently, decreasing the over-recruitment of primordial follicles after chemotherapy. It is worth mentioning that Kano *et al.* (2017) have recently shown that treatment with AMH during antitumoral therapies (carboplatin, doxorubicin and Cy) can protect the ovarian reserve in mice (Kano *et al.*, 2017). However, we cannot disregard that C1P may be preventing primordial follicle activation by other

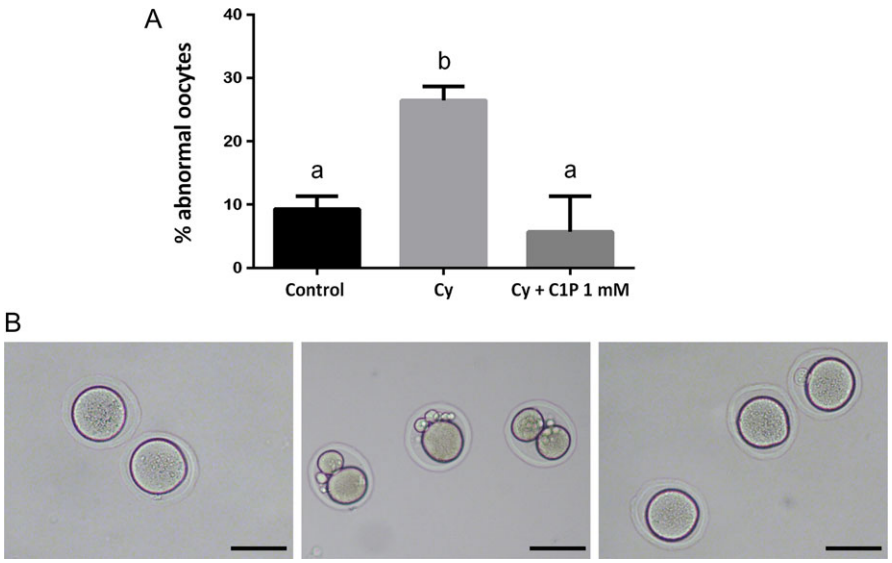

Figure 8 Ceramide-1-phosphate (C1P) protects oocytes from cyclophosphamide (Cy)-induced anomalies. (**A**) Quantification of abnormal oocytes, calculated as a percentage of abnormal oocytes/total recovered oocytes per each animal. Statistical analyses were performed by one-way ANOVA followed by Tukey's multiple-comparison test. Different letters represent statistically significant differences between groups (a vs b: $P < 0.05$), whereas means that share the same letter do not differ significantly. (**B**) Representative photomicrographs of abnormal oocytes from control, Cy-treated and Cy + C1P-treated mice. Scale bar represents 100 μm.

mechanisms and therefore AMH levels increase due to higher number of small follicles expressing AMH. Further experiments are required to elucidate these hypotheses.

It is known that Cy causes ovarian dysfunction by increasing apoptosis and alteration of folliculogenesis and thus, affecting steroid hormone secretion (Ataya *et al.*, 1989). Additionally, it has been reported that dose-dependent ovarian toxicity induced by Cy generates widespread loss of the follicles of the earliest stages, associated with reduction in estradiol levels (Jarrell *et al.*, 1987). In our study, the results showed that treatment with C1P reduced serum FSH and increased ovarian tissue E2 concentrations in Cy-treated mice. Since chemotherapy causes severe alterations in folliculogenesis by inducing hypogonadism, as observed by high levels of FSH and low levels of E2 (Bines *et al.*, 1996), our results suggest that C1P has protective properties against Cy-induced ovarian damage.

Along with our study, several other studies have determined that Cy induces atresia, severely affecting follicular development in the ovary (Bokser *et al.*, 1990; Jarrell *et al.*, 1991). Additionally, Cy causes apoptosis and induces oxidative stress in ovarian cells (Tsai-Turton *et al.*, 2007). Since Cy has a strong effect on proliferating cells, granulosa cells in growing follicles (preantral and antral follicles) are key targets for this drug, inducing apoptosis in these follicular stages. In our study, we showed that the percentage of TUNEL-positive cells was lower in preantral and early antral follicles from Cy + C1P mice compared to the Cy group. These results were also consistent with those from the cleaved caspase-3 immunostaining. Interestingly, we have found no evidence that Cy-induced depletion of primordial follicles is due to apoptosis. Cy could indeed trigger follicle activation and growth, causing a 'burnout' phenomenon and depletion of the ovarian reserve (Kalich-Philosoph *et al.*, 2013; Roness *et al.*, 2013). Histological studies have shown absence of apoptosis in primordial follicles and presence of apoptosis in large follicles after chemotherapy. The 'burnout' phenomenon has been well described by several knock-out mouse models (Adhikari *et al.*, 2009, 2010), as well as by *in-vitro* studies on human cortical tissue (Li *et al.*, 2010; Kawamura *et al.*, 2013). It has also been demonstrated that activation of primordial follicles is mediated by up-regulation of the PI3K/PTEN/Akt signaling pathway. Cy may induce activation of the PI3K/PTEN/Akt pathway via direct effects on the oocytes and pregranulosa cells of primordial follicles, or indirectly via Cy-induced destruction of larger follicles (Roness, 2013).

Ovarian cells exposed to Cy undergo apoptosis through intrinsic pathway mechanisms and present a dysregulation in the expression of BCL-2 family members. Additionally, Cy causes the activation of caspase-3, being the principal downstream effector enzyme in apoptosis process (Fu *et al.*, 2008; Strauss *et al.*, 2008; Zhao *et al.*, 2010). In our experimental model, ovaries obtained from Cy-treated mice showed a decrease in BCLX-L (antiapoptotic factor) and an increase in BAX (proapoptotic factor) protein levels. However, local administration of C1P was able to restore these protein levels to control values, compared to Cy-treated mice. In agreement with these observations, Gómez Muñoz *et al.* (2005) have shown that C1P enhances the expression of antiapoptotic BCLX-L isoform and inhibits cell death in primary bone marrow-derived macrophages (BMDM) under apoptotic conditions (Gómez Muñoz *et al.*, 2005). Still, few studies have evaluated the antiapoptotic function of C1P. Mitra *et al.* (2007) have shown that down-regulation of CerK in mammalian cells induces apoptosis and decreases growth (Mitra *et al.*, 2007). As mentioned above, Gómez Muñoz *et al.* (2004) have shown the antiapoptotic role of C1P in BMDM, which specifically involved direct inhibition of acid sphingomyelinase (A-SMase) and, in turn, a decrease in ceramide levels and

inhibition of the caspase 9/caspase-3 pathway (Gómez Muñoz *et al.*, 2004). In our study, we demonstrated that Cy caused an increase in A-SMase levels compared to the control group. Nonetheless, C1P decreased this protein expression levels compared to Cy-treated ovaries. These results suggest that C1P was able to indirectly decrease ceramide levels through the blockade of A-SMase in the Cy-treated ovary. In addition, the decrease we have demonstrated in cleaved caspase-3 expression in Cy + C1P ovaries is in agreement with these results.

Many studies have shown the impact of chemotherapy on vascular system in the ovary. Histological analysis has shown indirect effects of cytotoxic treatments through stromal cell damage (Doll *et al.*, 1986). It has been demonstrated that after *in-vivo* administration of doxorubicin there is a significant decrease in ovarian blood volume and a narrowing of blood vessels (Bar-Joseph *et al.*, 2011). Regarding vWF, lectin and α-SMA staining of vessels, Cy treatment caused an endothelial injury and altered vascular stability in the ovary and C1P was able to decrease the stromal damage caused by chemotherapy. These results are consistent with previous data observed by other investigators who have demonstrated that chemotherapy causes stromal fibrosis and disorganized and immature blood vessels in the ovarian cortex (Marcello *et al.*, 1990; Meirow *et al.*, 2007). It is noteworthy that C1P can be released upon tissue damage and regulates migration of stromal and endothelial cells and induction of *in-vivo* angiogenesis. C1P could be a candidate to improve vascular function in the ovary during chemotherapy (Kim *et al.*, 2013). In this regard, while the primordial and primary follicles obtain oxygen and nutrients by passive diffusion from blood vessels found in the ovarian cortex, which is an area scarce in vessels, the preantral and antral follicles possess their own individual capillary networks and are frequently found in blood vessel-rich areas. In this context, the beneficial effects of C1P concerning vascularization are especially decisive for the viability of the smallest follicles. C1P could decrease ovarian vascular injury and therefore protect ovarian reserve via its effect on blood vessels. More studies are needed to elucidate this point.

Another reproductive organ damaged by Cy is the uterus, which has proliferative activity in the growing grandular epithelium and in the stroma from endometrium. Thus, Cy also exerts cytotoxic effects on these tissues. Plowchalk *et al.* (1992) have shown that this chemotherapeutic agent caused a decrease in uterine weight in response to the toxicity in the ovary. In the current study, we observed that treatment with Cy critically affected the epithelial and stromal compartments and, additionally, the presence of glandular branches was reduced. However, C1P protected the endometrial tissues from this effect, hampering the loss of stromal quality and its glandular branches. These results suggest that C1P could enhance uterine morphology in Cy-treated mice. Plowchalk *et al.* (1992) have suggested that Cy-treated mice present reduced uterine weight due to alterations in the uterine responsiveness to sex steroids. Based on these data, C1P could be acting as a cytoprotective agent in the uterus, avoiding possible modifications in the hormone receptors and/or toxicity to endometrial cells.

Furthermore, C1P administration prolonged the fertile period following Cy treatment, since it prevented the decrease in pregnancy rates and in the number of offspring produced, lessening the effects observed in Cy-treated mice at the longer periods of time. This is consistent with the preservation of the primordial follicle pool and could represent a potential delay or protection from the onset of POF in chemotherapy patients.

As for IVF studies, there were no significant differences among groups except for an increase in the percentage of abnormal oocytes in Cy-treated mice, which C1P prevented. Normal oocytes from all groups were fertilized and developed into blastocysts in a similar manner, which suggests that patients under Cy-induced gonadotoxic effects may still experience restored fertility if their ovarian reserve is protected from depletion.

In the present study, intrabursal administration of C1P has been carried out to obtain a local antiapoptotic and proangiogenic effect. In order to disregard interaction between antitumoral therapies and the actions of this sphingolipid, more studies are required in both *in-vitro* and *in-vivo* animal models. Bittman and collaborators have synthesized specific photosensitive caged C1P analogues that can be released into the cytosol upon light irradiation in a specific tissue such as the ovary (Lankalapalli *et al.*, 2009; Gomez-Munoz *et al.*, 2016). In the future, this type of novel strategy would represent an adequate way of local administration of C1P in the ovary.

In summary, our study shows that local C1P administration drastically reduces Cy-induced damage in the ovary via protection of follicular reserve, restoration of hormone levels, diminution of apoptosis and improvement of stromal vasculature. Furthermore, C1P prevents deterioration of the uterine morphology caused by chemotherapy and protects fertility and oocyte quality.

Although further studies are necessary to corroborate C1P effectivity in humans, the future development of C1P agonists and their subsequent oral administration before Cy treatments might be a promising fertility-sparing strategy in female cancer patients whose reproductive function is at risk.

Further studies on C1P effects on female reproduction in pathological conditions such as chemotherapy-induced ovarian failure and on the safety of use of this sphingolipid are required.

Acknowledgements

We thank the Williams Foundation and René Barón Foundation, Argentina, for their valuable contribution of equipment to this study.

Authors' role

N.P. performed the experiments, analysed and interpreted the data and contributed in article drafting. L.S. discussed the results and contributed in article drafting. M.D.P. and G.O. contributed to data interpretation and discussed the results. D.B. executed the hormone assays and assisted in data analysis. M.M. performed the histological analyses of ovarian vasculature and uterine morphology. P.S.C. and D.J.C. contributed to design, analysis and interpretation of the fertility and oocyte quality experiments. A.G.M. contributed in the article drafting. M.T. and D.A. analysed and discussed the results, and contributed in the article drafting. F.P. conceived the concept, designed the experiments, supervised the study and wrote the article. All the authors read and approved the final article.

Funding

Grants Agencia Nacional de Promoción Científica y Tecnologica (PICT 2015-1117), Consejo Nacional de Investigaciones Científicas y Técnicas

(PIP 380), Argentinian National Cancer Institute and A. J. Roemmers Foundation, Argentina.

Conflict of interest

The authors declare no potential conflicts of interest with respect to the research, authorship, and/or publication of this article.

References

Adhikari D, Flohr G, Gorre N, Shen Y, Yang H, Lundin E, Lan Z, Gambello MJ, Liu K. Disruption of Tsc2 in oocytes leads to overactivation of the entire pool of primordial follicles. *Mol Hum Reprod* 2009;**15**:765–770.

Adhikari D, Zheng W, Shen Y, Gorre N, Hamalainen T, Cooney AJ, Huhtaniemi I, Lan ZJ, Liu K. Tsc/mTORC1 signaling in oocytes governs the quiescence and activation of primordial follicles. *Hum Mol Genet* 2010;**19**:397–410.

Anderson RA, Cameron DA. Pretreatment serum anti-mullerian hormone predicts long-term ovarian function and bone mass after chemotherapy for early breast cancer. *J Clin Endocrinol Metab* 2011;**96**:1336–1343.

Andreu C, Parborell F, Vanzulli S, Chemes H, Tesone M. Regulation of follicular luteinization by a gonadotropin-releasing hormone agonist: relationship between steroidogenesis and apoptosis. *Mol Reprod Dev* 1998;**51**:287–294.

Abir R, Ben-Haroush A, Felz C, Okon E, Raanani H, Orvieto R, Nitke S, Fisch B. Selection of patients before and after anticancer treatment for ovarian cryopreservation. *Hum Reprod* 2008;**23**:869–877.

Arana L, Gangoiti P, Ouro A, Trueba M, Gomez-Munoz A. Ceramide and ceramide 1-phosphate in health and disease. *Lipids Health Dis* 2010;**9**:15.

Arana L, Ordonez M, Ouro A, Rivera IG, Gangoiti P, Trueba M, Gomez-Munoz A. Ceramide 1-phosphate induces macrophage chemoattractant protein-1 release: involvement in ceramide 1-phosphate-stimulated cell migration. *Am J Physiol Endocrinol Metab* 2013;**304**:E1213–E1226.

Ataya KM, Pydyn EF, Sacco AG. Effect of 'activated' cyclophosphamide on mouse oocyte in vitro fertilization and cleavage. *Reprod Toxicol* 1988;**2**:105–109.

Ataya KM, Valeriote FA, Ramahi-Ataya AJ. Effect of cyclophosphamide on the immature rat ovary. *Cancer Res* 1989;**49**:1660–1664.

Augustin HG, Braun K, Telemenakis I, Modlich U, Kuhn W. Ovarian angiogenesis. Phenotypic characterization of endothelial cells in a physiological model of blood vessel growth and regression. *Am J Pathol* 1995;**147**:339–351.

Bar-Joseph H, Ben-Aharon I, Tzabari M, Tsarfaty G, Stemmer SM, Shalgi R. In vivo bioimaging as a novel strategy to detect doxorubicin-induced damage to gonadal blood vessels. *PLoS One* 2011;**6**:e23492.

Bildik G, Akin N, Senbabaoglu F, Sahin GN, Karahuseyinoglu S, Ince U, Taskiran C, Selek U, Yakin K, Guzel Y *et al*. GnRH agonist leuprolide acetate does not confer any protection against ovarian damage induced by chemotherapy and radiation in vitro. *Hum Reprod* 2015;**30**:2912–2925.

Bines J, Oleske DM, Cobleigh MA. Ovarian function in premenopausal women treated with adjuvant chemotherapy for breast cancer. *J Clin Oncol* 1996;**14**:1718–1729.

Blumenfeld Z, Avivi I, Ritter M, Rowe JM. Preservation of fertility and ovarian function and minimizing chemotherapy-induced gonadotoxicity in young women. *J Soc Gynecol Investig* 1999;**6**:229–239.

Blumenfeld Z, von Wolff M. GnRH-analogues and oral contraceptives for fertility preservation in women during chemotherapy. *Hum Reprod Update* 2008;**14**:543–552.

Blumenfeld Z, Zur H, Dann EJ. Gonadotropin-releasing hormone agonist cotreatment during chemotherapy may increase pregnancy rate in survivors. *Oncologist* 2015;**20**:1283–1289.

Bokser L, Szende B, Schally AV. Protective effects of D-Trp6-luteinising hormone-releasing hormone microcapsules against cyclophosphamide-induced gonadotoxicity in female rats. *Br J Cancer* 1990;**61**:861–865.

Castrillon DH, Miao L, Kollipara R, Horner JW, DePinho RA. Suppression of ovarian follicle activation in mice by the transcription factor Foxo3a. *Science* 2003;**301**:215–218.

Cherry JA, Hou X, Rueda BR, Davis JS, Townson DH. Microvascular endothelial cells of the bovine corpus luteum: a comparative examination of the estrous cycle and pregnancy. *J Reprod Dev* 2008;**54**:183–191.

Cuvillier O, Pirianov G, Kleuser B, Vanek PG, Coso OA, Gutkind S, Spiegel S. Suppression of ceramide-mediated programmed cell death by sphingosine-1-phosphate. *Nature* 1996;**381**:800–803.

Desmeules P, Devine PJ. Characterizing the ovotoxicity of cyclophosphamide metabolites on cultured mouse ovaries. *Toxicol Sci* 2006;**90**:500–509.

Di Giorgio NP, Catalano PN, Lopez PV, Gonzalez B, Semaan SJ, Lopez GC, Kauffman AS, Rulli SB, Somoza GM, Bettler B *et al*. Lack of functional GABAB receptors alters Kiss1, Gnrh1 and Gad1 mRNA expression in the medial basal hypothalamus at postnatal day 4. *Neuroendocrinology* 2013;**98**:212–223.

Di Pietro M, Pascuali N, Scotti L, Irusta G, Bas D, May M, Tesone M, Abramovich D, Parborell F. In vivo intrabursal administration of bioactive lipid sphingosine-1-phosphate enhances vascular integrity in a rat model of ovarian hyperstimulation syndrome. *Mol Hum Reprod* 2017;**23**:417–427.

Doll DC, Ringenberg QS, Yarbro JW. Vascular toxicity associated with antineoplastic agents. *J Clin Oncol* 1986;**4**:1405–1417.

D'Herde K, De Pestel G, Roels F. In situ end labeling of fragmented DNA in induced ovarian atresia. *Biochem Cell Biol* 1994;**72**:573–579.

Durlinger AL, Kramer P, Karels B, de Jong FH, Uilenbroek JT, Grootegoed JA, Themmen AP. Control of primordial follicle recruitment by anti-Mullerian hormone in the mouse ovary. *Endocrinology* 1999;**140**:5789–5796.

Falcone T, Bedaiwy MA. Fertility preservation and pregnancy outcome after malignancy. *Curr Opin Obstet Gynecol* 2005;**17**:21–26.

Familiari G, Caggiati A, Nottola SA, Ermini M, Di Benedetto MR, Motta PM. Ultrastructure of human ovarian primordial follicles after combination chemotherapy for Hodgkin's disease. *Hum Reprod* 1993;**8**:2080–2087.

Fu X, He Y, Xie C, Liu W. Bone marrow mesenchymal stem cell transplantation improves ovarian function and structure in rats with chemotherapy-induced ovarian damage. *Cytotherapy* 2008;**10**:353–363.

Fujiwara Y, Komiya T, Kawabata H, Sato M, Fujimoto H, Furusawa M, Noce T. Isolation of a DEAD-family protein gene that encodes a murine homolog of Drosophila vasa and its specific expression in germ cell lineage. *Proc Natl Acad Sci USA* 1994;**91**:12258–12262.

Gangoiti P, Arana L, Ouro A, Granado MH, Trueba M, Gomez-Munoz A. Activation of mTOR and RhoA is a major mechanism by which Ceramide 1-phosphate stimulates macrophage proliferation. *Cell Signal* 2011;**23**:27–34.

Gangoiti P, Bernacchioni C, Donati C, Cencetti F, Ouro A, Gomez-Munoz A, Bruni P. Ceramide 1-phosphate stimulates proliferation of C2C12 myoblasts. *Biochimie* 2012;**94**:597–607.

Gangoiti P, Camacho L, Arana L, Ouro A, Granado MH, Brizuela L, Casas J, Fabrias G, Abad JL, Delgado A *et al*. Control of metabolism and signaling of simple bioactive sphingolipids: implications in disease. *Prog Lipid Res* 2010;**49**:316–334.

Gomez-Elias MD, Munuce MJ, Bahamondes L, Cuasnicu PS, Cohen DJ. In vitro and in vivo effects of ulipristal acetate on fertilization and early embryo development in mice. *Hum Reprod* 2016;**31**:53–59.

Gomez-Munoz A, Duffy PA, Martin A, O'Brien L, Byun HS, Bittman R, Brindley DN. Short-chain ceramide-1-phosphates are novel stimulators of DNA synthesis and cell division: antagonism by cell-permeable ceramides. *Mol Pharmacol* 1995;**47**:833–839.

Gomez-Munoz A, Gangoiti P, Arana L, Ouro A, Rivera IG, Ordonez M, Trueba M. New insights on the role of ceramide 1-phosphate in inflammation. *Biochim Biophys Acta* 2013;**1831**:1060–1066.

Gomez-Munoz A, Gangoiti P, Rivera IG, Presa N, Gomez-Larrauri A, Ordonez M. Caged ceramide 1-phosphate (C1P) analogs: novel tools for studying C1P biology. *Chem Phys Lipids* 2016;**194**:79–84.

Gonfloni S, Di Tella L, Caldarola S, Cannata SM, Klinger FG, Di Bartolomeo C, Mattei M, Candi E, De Felici M, Melino G *et al*. Inhibition of the c-Abl-TAp63 pathway protects mouse oocytes from chemotherapy-induced death. *Nature Med* 2009;**15**:1179–1185.

Gómez Muñoz A, Kong JY, Parhar K, Wang SW, Gangoiti P, Gonzalez M, Eivemark S, Salh B, Duronio V, Steinbrecher UP. Ceramide-1-phosphate promotes cell survival through activation of the phosphatidylinositol 3-kinase/protein kinase B pathway. *FEBS Lett* 2005;**579**:3744–3750.

Gómez Muñoz A, Kong JY, Salh B, Steinbrecher UP. Ceramide-1-phosphate blocks apoptosis through inhibition of acid sphingomyelinase in macrophages. *J Lipid Res* 2004;**45**:99–105.

Hancke K, Strauch O, Kissel C, Gobel H, Schafer W, Denschlag D. Sphingosine 1-phosphate protects ovaries from chemotherapy-induced damage in vivo. *Fertil Steril* 2007;**87**:172–177.

Himelstein-Braw R, Peters H, Faber M. Morphological study of the ovaries of leukaemic children. *Br J Cancer* 1978;**38**:82–87.

Irusta G, Parborell F, Tesone M. Inhibition of cytochrome P-450 C17 enzyme by a GnRH agonist in ovarian follicles from gonadotropin-stimulated rats. *Am J Physiol Endocrinol Metab* 2007;**292**:E1456–E1464.

Jarrell JF, Bodo L, YoungLai EV, Barr RD, O'Connell GJ. The short-term reproductive toxicity of cyclophosphamide in the female rat. *Reprod Toxicol* 1991;**5**:481–485.

Jarrell J, Lai EV, Barr R, McMahon A, Belbeck L, O'Connell G. Ovarian toxicity of cyclophosphamide alone and in combination with ovarian irradiation in the rat. *Cancer Res* 1987;**47**:2340–2343.

Jurisicova A, Lee HJ, D'Estaing SG, Tilly J, Perez GI. Molecular requirements for doxorubicin-mediated death in murine oocytes. *Cell Death Differ* 2006;**13**:1466–1474.

Kalich-Philosoph L, Roness H, Carmely A, Fishel-Bartal M, Ligumsky H, Paglin S, Wolf I, Kanety H, Sredni B, Meirow D. Cyclophosphamide triggers follicle activation and 'burnout'; AS101 prevents follicle loss and preserves fertility. *Sci Transl Med* 2013;**5**:185ra162.

Kano M, Sosulski AE, Zhang L, Saatcioglu HD, Wang D, Nagykery N, Sabatini ME, Gao G, Donahoe PK, Pepin D. AMH/MIS as a contraceptive that protects the ovarian reserve during chemotherapy. *Proc Natl Acad Sci USA* 2017;**114**:E1688–E1697.

Kawamura K, Cheng Y, Suzuki N, Deguchi M, Sato Y, Takae S, Ho CH, Kawamura N, Tamura M, Hashimoto S *et al*. Hippo signaling disruption and Akt stimulation of ovarian follicles for infertility treatment. *Proc Natl Acad Sci USA* 2013;**110**:17474–17479.

Kaya H, Desdicioglu R, Sezik M, Ulukaya E, Ozkaya O, Yilmaztepe A, Demirci M. Does sphingosine-1-phosphate have a protective effect on cyclophosphamide- and irradiation-induced ovarian damage in the rat model? *Fertil Steril* 2008;**89**:732–735.

Kim SY, Ebbert K, Cordeiro MH, Romero M, Zhu J, Serna VA, Whelan KA, Woodruff TK, Kurita T. Cell autonomous phosphoinositide 3-kinase activation in oocytes disrupts normal ovarian function through promoting survival and overgrowth of ovarian follicles. *Endocrinology* 2015;**156**:1464–1476.

Kim C, Schneider G, Abdel-Latif A, Mierzejewska K, Sunkara M, Borkowska S, Ratajczak J, Morris AJ, Kucia M, Ratajczak MZ. Ceramide-1-phosphate regulates migration of multipotent stromal cells and endothelial progenitor cells—implications for tissue regeneration. *Stem Cells* 2013;**31**:500–510.

La Marca A, Broekmans FJ, Volpe A, Fauser BC, Macklon NS. Table ESIGfRE—AR. Anti-Mullerian hormone (AMH): what do we still need to know? *Hum Reprod* 2009;**24**:2264–2275.

Lankalapalli RS, Ouro A, Arana L, Gomez-Munoz A, Bittman R. Caged ceramide 1-phosphate analogues: synthesis and properties. *J Org Chem* 2009;**74**:8844–8847.

Li J, Kawamura K, Cheng Y, Liu S, Klein C, Liu S, Duan EK, Hsueh AJ. Activation of dormant ovarian follicles to generate mature eggs. *Proc Natl Acad Sci U S A* 2010;**107**:10280–10284.

Li F, Turan V, Lierman S, Cuvelier C, De Sutter P, Oktay K. Sphingosine-1-phosphate prevents chemotherapy-induced human primordial follicle death. *Hum Reprod* 2014;**29**:107–113.

Maceyka M, Payne SG, Milstien S, Spiegel S. Sphingosine kinase, sphingosine-1-phosphate, and apoptosis. *Biochim Biophys Acta* 2002;**1585**:193–201.

Marcello MF, Nuciforo G, Romeo R, Di Dino G, Russo I, Russo A, Palumbo G, Schiliro G. Structural and ultrastructural study of the ovary in childhood leukemia after successful treatment. *Cancer* 1990;**66**:2099–2104.

Mark-Kappeler CJ, Hoyer PB, Devine PJ. Xenobiotic effects on ovarian preantral follicles. *Biol Reprod* 2011;**85**:871–883.

Meirow D, Dor J, Kaufman B, Shrim A, Rabinovici J, Schiff E, Raanani H, Levron J, Fridman E. Cortical fibrosis and blood-vessels damage in human ovaries exposed to chemotherapy. Potential mechanisms of ovarian injury. *Hum Reprod* 2007;**22**:1626–1633.

Meirow D, Epstein M, Lewis H, Nugent D, Gosden RG. Administration of cyclophosphamide at different stages of follicular maturation in mice: effects on reproductive performance and fetal malformations. *Hum Reprod* 2001;**16**:632–637.

Meirow D, Nugent D. The effects of radiotherapy and chemotherapy on female reproduction. *Hum Reprod Update* 2001;**7**:535–543.

Mitra P, Maceyka M, Payne SG, Lamour N, Milstien S, Chalfant CE, Spiegel S. Ceramide kinase regulates growth and survival of A549 human lung adenocarcinoma cells. *FEBS Lett* 2007;**581**:735–740.

Morita Y, Perez GI, Paris F, Miranda SR, Ehleiter D, Haimovitz-Friedman A, Fuks Z, Xie Z, Reed JC, Schuchman EH *et al*. Oocyte apoptosis is suppressed by disruption of the acid sphingomyelinase gene or by sphingosine-1-phosphate therapy. *Nature Med* 2000;**6**:1109–1114.

Morita Y, Tilly JL. Sphingolipid regulation of female gonadal cell apoptosis. *Ann N Y Acad Sci* 2000;**905**:209–220.

Niwa S, Graf C, Bornancin F. Ceramide kinase deficiency impairs microendothelial cell angiogenesis in vitro. *Microvasc Res* 2009;**77**:389–393.

Oktem O, Oktay K. Quantitative assessment of the impact of chemotherapy on ovarian follicle reserve and stromal function. *Cancer* 2007;**110**:2222–2229.

Ouro A, Arana L, Rivera IG, Ordonez M, Gomez-Larrauri A, Presa N, Simon J, Trueba M, Gangoiti P, Bittman R *et al*. Phosphatidic acid inhibits ceramide 1-phosphate-stimulated macrophage migration. *Biochem Pharmacol* 2014;**92**:642–650.

Paris F, Perez GI, Fuks Z, Haimovitz-Friedman A, Nguyen H, Bose M, Ilagan A, Hunt PA, Morgan WF, Tilly JL *et al*. Sphingosine 1-phosphate preserves fertility in irradiated female mice without propagating genomic damage in offspring. *Nature Med* 2002;**8**:901–902.

Pascuali N, Scotti L, Abramovich D, Irusta G, Di Pietro M, Bas D, Tesone M, Parborell F. Inhibition of platelet-derived growth factor (PDGF) receptor affects follicular development and ovarian proliferation, apoptosis and angiogenesis in prepubertal eCG-treated rats. *Mol Cell Endocrinol* 2015;**412**:148–158.

Perez GI, Knudson CM, Leykin L, Korsmeyer SJ, Tilly JL. Apoptosis-associated signaling pathways are required for chemotherapy-mediated female germ cell destruction. *Nature Med* 1997;**3**:1228–1232.

Petrillo SK, Desmeules P, Truong TQ, Devine PJ. Detection of DNA damage in oocytes of small ovarian follicles following phosphoramide mustard exposures of cultured rodent ovaries in vitro. *Toxicol Appl Pharmacol* 2011;**253**:94–102.

Plowchalk DR, Meadows MJ, Mattison DR. Reproductive toxicity of cyclophosphamide in the C57BL/6N mouse: 2. Effects on uterine structure and function. *Reprod Toxicol* 1992;**6**:423–429.

Pydyn EF, Ataya KM. Effect of cyclophosphamide on mouse oocyte in vitro fertilization and cleavage: recovery. *Reprod Toxicol* 1991;**5**:73–78.

Qi X, Okamoto Y, Murakawa T, Wang F, Oyama O, Ohkawa R, Yoshioka K, Du W, Sugimoto N, Yatomi Y *et al*. Sustained delivery of sphingosine-1-phosphate using poly(lactic-co-glycolic acid)-based microparticles stimulates Akt/ERK-eNOS mediated angiogenesis and vascular maturation restoring blood flow in ischemic limbs of mice. *Eur J Pharmacol* 2010; **634**:121–131.

Raz A, Fisch B, Okon E, Feldberg D, Nitke S, Raanani H, Abir R. Possible direct cytoxicity effects of cyclophosphamide on cultured human follicles: an electron microscopy study. *J Assist Reprod Genet* 2002;**19**:500–506.

Redmer DA, Doraiswamy V, Bortnem BJ, Fisher K, Jablonka-Shariff A, Grazul-Bilska AT, Reynolds LP. Evidence for a role of capillary pericytes in vascular growth of the developing ovine corpus luteum. *Biol Reprod* 2001;**65**:879–889.

Rivera IG, Ordonez M, Presa N, Gomez-Larrauri A, Simon J, Trueba M, Gomez-Munoz A. Sphingomyelinase D/ceramide 1-phosphate in cell survival and inflammation. *Toxins* 2015;**7**:1457–1466.

Roness H. Cyclophosphamide triggers follicle activation causing ovarian reserve'burnout'; AS101 preserves fertility. *ESHRE*. 2013, London, UK.

Roness H, Gavish Z, Cohen Y, Meirow D. Ovarian follicle burnout: a universal phenomenon? *Cell Cycle* 2013;**12**:3245–3246.

Rosendahl M, Andersen CY, la Cour Freiesleben N, Juul A, Lossl K, Andersen AN. Dynamics and mechanisms of chemotherapy-induced ovarian follicular depletion in women of fertile age. *Fertil Steril* 2010;**94**:156–166.

Rossi V, Lispi M, Longobardi S, Mattei M, Rella FD, Salustri A, De Felici M, Klinger FG. LH prevents cisplatin-induced apoptosis in oocytes and preserves female fertility in mouse. *Cell Death Differ* 2017;**24**:72–82.

Sanchez AM, Giorgione V, Vigano P, Papaleo E, Candiani M, Mangili G, Panina-Bordignon P. Treatment with anticancer agents induces dysregulation of specific Wnt signaling pathways in human ovarian luteinized granulosa cells in vitro. *Toxicol Sci* 2013;**136**:183–192.

Schmidt D, Ovitt CE, Anlag K, Fehsenfeld S, Gredsted L, Treier AC, Treier M. The murine winged-helix transcription factor Foxl2 is required for granulosa cell differentiation and ovary maintenance. *Development* 2004; **131**:933–942.

Scotti L, Abramovich D, Pascuali N, Irusta G, Meresman G, Tesone M, Parborell F. Local VEGF inhibition prevents ovarian alterations associated with ovarian hyperstimulation syndrome. *J Steroid Biochem Mol Biol* 2014; **144 Pt B**:392–401.

Scotti L, Di Pietro M, Pascuali N, Irusta G, de Zuniga I, Gomez Pena M, Pomilio C, Saravia F, Tesone M, Abramovich D *et al*. Sphingosine-1-phosphate restores endothelial barrier integrity in ovarian hyperstimulation syndrome. *Mol Hum Reprod* 2016;**22**:852–866.

Scotti L, Irusta G, Abramovich D, Tesone M, Parborell F. Administration of a gonadotropin-releasing hormone agonist affects corpus luteum vascular stability and development and induces luteal apoptosis in a rat model of ovarian hyperstimulation syndrome. *Mol Cell Endocrinol* 2011;**335**:116–125.

Stefansdottir A, Fowler PA, Powles-Glover N, Anderson RA, Spears N. Use of ovary culture techniques in reproductive toxicology. *Reprod Toxicol* 2014;**49**:117–135.

Strauss G, Westhoff MA, Fischer-Posovszky P, Fulda S, Schanbacher M, Eckhoff SM, Stahnke K, Vahsen N, Kroemer G, Debatin KM. 4-hydroperoxy-cyclophosphamide mediates caspase-independent T-cell apoptosis involving oxidative stress-induced nuclear relocation of mitochondrial apoptogenic factors AIF and EndoG. *Cell Death Differ* 2008;**15**: 332–343.

Tilly JL. Ovarian follicle counts—not as simple as 1, 2, 3. *Reprod Biol Endocrinol* 2003;**1**:11.

Tsai-Turton M, Luong BT, Tan Y, Luderer U. Cyclophosphamide-induced apoptosis in COV434 human granulosa cells involves oxidative stress and glutathione depletion. *Toxicol Sci* 2007;**98**:216–230.

Wallace WH, Kelsey TW. Human ovarian reserve from conception to the menopause. *PLoS One* 2010;**5**:e8772.

Zhao XJ, Huang YH, Yu YC, Xin XY. GnRH antagonist cetrorelix inhibits mitochondria-dependent apoptosis triggered by chemotherapy in granulosa cells of rats. *Gynecol Oncol* 2010;**118**:69–75.